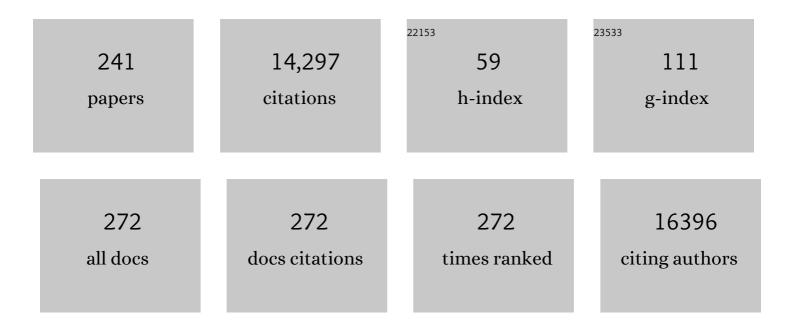
Junliang Sun

List of Publications by Year in descending order

Source: https://exaly.com/author-pdf/9131776/publications.pdf Version: 2024-02-01



LUNLIANC SUN

#	Article	IF	CITATIONS
1	Single-crystal x-ray diffraction structures of covalent organic frameworks. Science, 2018, 361, 48-52.	12.6	868
2	Thermochromic halide perovskite solar cells. Nature Materials, 2018, 17, 261-267.	27.5	630
3	The ITQ-37 mesoporous chiral zeolite. Nature, 2009, 458, 1154-1157.	27.8	526
4	Achieving High Pseudocapacitance of 2D Titanium Carbide (MXene) by Cation Intercalation and Surface Modification. Advanced Energy Materials, 2017, 7, 1602725.	19.5	514
5	Selectivity and direct visualization of carbon dioxide and sulfur dioxide in a decorated porous host. Nature Chemistry, 2012, 4, 887-894.	13.6	466
6	Ultrafast epitaxial growth of metre-sized single-crystal graphene on industrial Cu foil. Science Bulletin, 2017, 62, 1074-1080.	9.0	454
7	Ba3Mg3(BO3)3F3 polymorphs with reversible phase transition and high performances as ultraviolet nonlinear optical materials. Nature Communications, 2018, 9, 3089.	12.8	314
8	Selfâ€5upporting Metal–Organic Layers as Singleâ€5ite Solid Catalysts. Angewandte Chemie - International Edition, 2016, 55, 4962-4966.	13.8	303
9	Pyrazolate-Based Porphyrinic Metal–Organic Framework with Extraordinary Base-Resistance. Journal of the American Chemical Society, 2016, 138, 914-919.	13.7	303
10	An AlEgen-based 3D covalent organic framework for white light-emitting diodes. Nature Communications, 2018, 9, 5234.	12.8	293
11	Three-dimensional rotation electron diffraction: software <i>RED</i> for automated data collection and data processing. Journal of Applied Crystallography, 2013, 46, 1863-1873.	4.5	264
12	Topologically guided tuning of Zr-MOF pore structures for highly selective separation of C6 alkane isomers. Nature Communications, 2018, 9, 1745.	12.8	251
13	Atomically precise single-crystal structures of electrically conducting 2D metal–organic frameworks. Nature Materials, 2021, 20, 222-228.	27.5	239
14	2D and 3D Porphyrinic Covalent Organic Frameworks: The Influence of Dimensionality on Functionality. Angewandte Chemie - International Edition, 2020, 59, 3624-3629.	13.8	227
15	Hierarchical Co(OH)F Superstructure Built by Lowâ€Đimensional Substructures for Electrocatalytic Water Oxidation. Advanced Materials, 2017, 29, 1700286.	21.0	227
16	Fine-Tuning of Crystal Packing and Charge Transport Properties of BDOPV Derivatives through Fluorine Substitution. Journal of the American Chemical Society, 2015, 137, 15947-15956.	13.7	224
17	Selective Adsorption of Sulfur Dioxide in a Robust Metal–Organic Framework Material. Advanced Materials, 2016, 28, 8705-8711.	21.0	214
18	A zeolite family with chiral and achiral structures built from the same building layer. Nature Materials, 2008, 7, 381-385.	27.5	205

#	Article	IF	CITATIONS
19	Structure and catalytic properties of the most complex intergrown zeolite ITQ-39 determined by electron crystallography. Nature Chemistry, 2012, 4, 188-194.	13.6	178
20	Reversible adsorption of nitrogen dioxide within a robust porous metal–organic framework. Nature Materials, 2018, 17, 691-696.	27.5	162
21	Atomically Dispersed Mo Supported on Metallic Co ₉ S ₈ Nanoflakes as an Advanced Nobleâ€Metalâ€Free Bifunctional Water Splitting Catalyst Working in Universal pH Conditions. Advanced Energy Materials, 2020, 10, 1903137.	19.5	162
22	An Iron-based Film for Highly Efficient Electrocatalytic Oxygen Evolution from Neutral Aqueous Solution. ACS Applied Materials & Interfaces, 2015, 7, 21852-21859.	8.0	161
23	The intrinsic properties of FA _(1â^'x) MA _x PbI ₃ perovskite single crystals. Journal of Materials Chemistry A, 2017, 5, 8537-8544.	10.3	152
24	Structural origin of the high-voltage instability of lithium cobalt oxide. Nature Nanotechnology, 2021, 16, 599-605.	31.5	148
25	Observation of Interpenetration Isomerism in Covalent Organic Frameworks. Journal of the American Chemical Society, 2018, 140, 6763-6766.	13.7	144
26	Facile Water-Based Strategy for Synthesizing MoO _{3–<i>x</i>} Nanosheets: Efficient Visible Light Photocatalysts for Dye Degradation. ACS Omega, 2018, 3, 2193-2201.	3.5	135
27	A tri-continuous mesoporous material with a silica pore wall following a hexagonal minimal surface. Nature Chemistry, 2009, 1, 123-127.	13.6	131
28	Cyclotricatechylene based porous crystalline material: Synthesis and applications in gas storage. Journal of Materials Chemistry, 2012, 22, 5369.	6.7	128
29	Isostructural Threeâ€Dimensional Covalent Organic Frameworks. Angewandte Chemie - International Edition, 2019, 58, 9770-9775.	13.8	126
30	Irreversible Network Transformation in a Dynamic Porous Host Catalyzed by Sulfur Dioxide. Journal of the American Chemical Society, 2013, 135, 4954-4957.	13.7	123
31	Emergent superconductivity in an iron-based honeycomb lattice initiated by pressure-driven spin-crossover. Nature Communications, 2018, 9, 1914.	12.8	119
32	<mml:math xmlns:mml="http://www.w3.org/1998/Math/MathML"><mml:mrow><mml:mrow><mml:mo>(</mml:mo><mml Ion-exchange synthesis of large single-crystal and highly two-dimensional electron. Physical Review B, 2015, 92, .</mml </mml:mrow></mml:mrow></mml:math 	:msyb> <mr 3.2</mr 	nl:mi>Li116
33	Seeded growth of large single-crystal copper foils with high-index facets. Nature, 2020, 581, 406-410.	27.8	116
34	A Crystalline Three-Dimensional Covalent Organic Framework with Flexible Building Blocks. Journal of the American Chemical Society, 2021, 143, 2123-2129.	13.7	105
35	Synthesis of an extra-large molecular sieve using proton sponges as organic structure-directing agents. Proceedings of the National Academy of Sciences of the United States of America, 2013, 110, 3749-3754.	7.1	103
36	Maximizing sinusoidal channels of HZSM-5 for high shape-selectivity to p-xylene. Nature Communications, 2019, 10, 4348.	12.8	102

#	Article	IF	CITATIONS
37	Organic hydrogen-bonded interpenetrating diamondoid frameworks from modular self-assembly of methanetetrabenzoic acid with linkers. CrystEngComm, 2009, 11, 978.	2.6	97
38	Highly Conducting Neutral Coordination Polymer with Infinite Two-Dimensional Silver–Sulfur Networks. Journal of the American Chemical Society, 2018, 140, 15153-15156.	13.7	97
39	Loneâ€Pair Enhanced Birefringence in an Alkalineâ€Earth Metal Tin(II) Phosphate BaSn ₂ (PO ₄) ₂ . Chemistry - A European Journal, 2019, 25, 5648-5651.	3.3	95
40	Pressure-Driven Cooperative Spin-Crossover, Large-Volume Collapse, and Semiconductor-to-Metal Transition in Manganese(II) Honeycomb Lattices. Journal of the American Chemical Society, 2016, 138, 15751-15757.	13.7	91
41	Zeolite A synthesized from alkaline assisted pre-activated halloysite for efficient heavy metal removal in polluted river water and industrial wastewater. Journal of Environmental Sciences, 2017, 56, 254-262.	6.1	91
42	Self-Assembly of Cetyltrimethylammonium Bromide and Lamellar Zeolite Precursor for the Preparation of Hierarchical MWW Zeolite. Chemistry of Materials, 2016, 28, 4512-4521.	6.7	88
43	Cage Based Crystalline Covalent Organic Frameworks. Journal of the American Chemical Society, 2019, 141, 3843-3848.	13.7	84
44	Tuning the Topology of Three-Dimensional Covalent Organic Frameworks via Steric Control: From pts to Unprecedented ljh . Journal of the American Chemical Society, 2021, 143, 7279-7284.	13.7	84
45	Highly crystalline covalent organic frameworks from flexible building blocks. Chemical Communications, 2016, 52, 4706-4709.	4.1	83
46	Twist Building Blocks from Planar to Tetrahedral for the Synthesis of Covalent Organic Frameworks. Journal of the American Chemical Society, 2020, 142, 3718-3723.	13.7	83
47	Synthesis and Structure of Polymorph B of Zeolite Beta. Chemistry of Materials, 2008, 20, 3218-3223.	6.7	80
48	Achieving Highly Efficient Catalysts for Hydrogen Evolution Reaction by Electronic State Modification of Platinum on Versatile Ti ₃ C ₂ T _{<i>x</i>} (MXene). ACS Sustainable Chemistry and Engineering, 2019, 7, 4266-4273.	6.7	79
49	Single crystal of a one-dimensional metallo-covalent organic framework. Nature Communications, 2020, 11, 1434.	12.8	77
50	EMM-23: A Stable High-Silica Multidimensional Zeolite with Extra-Large Trilobe-Shaped Channels. Journal of the American Chemical Society, 2014, 136, 13570-13573.	13.7	71
51	A Germanosilicate Structure with 11×11×12â€Ring Channels Solved by Electron Crystallography. Angewandte Chemie - International Edition, 2014, 53, 5868-5871.	13.8	69
52	Application of X-ray Diffraction and Electron Crystallography for Solving Complex Structure Problems. Accounts of Chemical Research, 2017, 50, 2737-2745.	15.6	69
53	Microporous Aluminoborates with Large Channels: Structural and Catalytic Properties. Angewandte Chemie - International Edition, 2011, 50, 12555-12558.	13.8	67
54	Thermally/hydrolytically stable covalent organic frameworks from a rigid macrocyclic host. Chemical Communications, 2014, 50, 788-791.	4.1	67

#	Article	IF	CITATIONS
55	A ₂ SnS ₅ : A Structural Incommensurate Modulation Exhibiting Strong Secondâ€Harmonic Generation and a High Laserâ€Induced Damage Threshold (A=Ba, Sr). Angewandte Chemie - International Edition, 2020, 59, 11861-11865.	13.8	67
56	Recent Advances in the Synthesis and Application of Twoâ€Dimensional Zeolites. Advanced Energy Materials, 2016, 6, 1600441.	19.5	65
57	Organic Semiconducting Alloys with Tunable Energy Levels. Journal of the American Chemical Society, 2019, 141, 6561-6568.	13.7	65
58	Electron Crystallography Reveals Atomic Structures of Metal–Organic Nanoplates with M ₁₂ (μ ₃ -O) ₈ (μ ₃ -OH) ₈ (μ _{-CH) (M = Zr, Hf) Secondary Building Units. Inorganic Chemistry, 2017, 56, 8128-8134.}	H)<4sudb>6∙	
59	3D Open-Framework Vanadoborate as a Highly Effective Heterogeneous Pre-catalyst for the Oxidation of Alkylbenzenes. Chemistry of Materials, 2013, 25, 5031-5036.	6.7	61
60	Self‣upporting Metal–Organic Layers as Single‣ite Solid Catalysts. Angewandte Chemie, 2016, 128, 5046-5050.	2.0	61
61	Nonâ€Interpenetrated Singleâ€Crystal Covalent Organic Frameworks. Angewandte Chemie - International Edition, 2020, 59, 17991-17995.	13.8	60
62	The Exploration of Carrier Behavior in the Inverted Mixed Perovskite Singleâ€Crystal Solar Cells. Advanced Materials Interfaces, 2018, 5, 1800224.	3.7	58
63	Processing Natural Wood into an Efficient and Durable Solar Steam Generation Device. ACS Applied Materials & Interfaces, 2020, 12, 18165-18173.	8.0	58
64	Multistep nucleation and growth mechanisms of organic crystals from amorphous solid states. Nature Communications, 2019, 10, 3872.	12.8	57
65	Molybdenum Oxide Nanosheets with Tunable Plasmonic Resonance: Aqueous Exfoliation Synthesis and Charge Storage Applications. Advanced Functional Materials, 2019, 29, 1806699.	14.9	55
66	Diverse crystal size effects in covalent organic frameworks. Nature Communications, 2020, 11, 6128.	12.8	55
67	Rational design of crystalline two-dimensional frameworks with highly complicated topological structures. Nature Communications, 2019, 10, 4609.	12.8	54
68	Diphosphine-induced chiral propeller arrangement of gold nanoclusters for singlet oxygen photogeneration. Nano Research, 2018, 11, 5787-5798.	10.4	53
69	Organocatalytic Highly Enantioselective Conjugate Addition of Aldehydes to Alkylidine Malonates. Advanced Synthesis and Catalysis, 2008, 350, 657-661.	4.3	52
70	Monodisperse Sandwich‣ike Coupled Quasiâ€Graphene Sheets Encapsulating Ni ₂ P Nanoparticles for Enhanced Lithiumâ€Ion Batteries. Chemistry - A European Journal, 2015, 21, 9229-9235.	3.3	50
71	Adsorption of Nitrogen Dioxide in a Redox-Active Vanadium Metal–Organic Framework Material. Journal of the American Chemical Society, 2020, 142, 15235-15239.	13.7	50
72	Immobilization of a Molecular Ruthenium Catalyst on Hematite Nanorod Arrays for Water Oxidation with Stable Photocurrent. ChemSusChem, 2015, 8, 3242-3247.	6.8	49

#	Article	IF	CITATIONS
73	Redox-triggered switching in three-dimensional covalent organic frameworks. Nature Communications, 2020, 11, 4919.	12.8	49
74	New Barium Cobaltite Series Ban+1ConO3n+3(Co8O8):  Intergrowth Structure Containing Perovskite and CdI2-Type Layers. Inorganic Chemistry, 2006, 45, 9151-9153.	4.0	48
75	Construction of Mesoporous Frameworks with Vanadoborate Clusters. Angewandte Chemie - International Edition, 2014, 53, 3608-3611.	13.8	46
76	Pressure-induced semiconductor-to-metal phase transition of a charge-ordered indium halide perovskite. Proceedings of the National Academy of Sciences of the United States of America, 2019, 116, 23404-23409.	7.1	45
77	2D and 3D Porphyrinic Covalent Organic Frameworks: The Influence of Dimensionality on Functionality. Angewandte Chemie, 2020, 132, 3653-3658.	2.0	45
78	Direct plasma phosphorization of Cu foam for Li ion batteries. Journal of Materials Chemistry A, 2020, 8, 16920-16925.	10.3	44
79	Tailoring the Pore Surface of 3D Covalent Organic Frameworks via Postâ€Synthetic Click Chemistry. Angewandte Chemie - International Edition, 2022, 61, .	13.8	44
80	Intergrown New Zeolite Beta Polymorphs with Interconnected 12-Ring Channels Solved by Combining Electron Crystallography and Single-Crystal X-ray Diffraction. Chemistry of Materials, 2012, 24, 3701-3706.	6.7	43
81	Adsorption Properties of MFM-400 and MFM-401 with CO ₂ and Hydrocarbons: Selectivity Derived from Directed Supramolecular Interactions. Inorganic Chemistry, 2016, 55, 7219-7228.	4.0	41
82	CsSiB ₃ O ₇ : A Beryllium-Free Deep-Ultraviolet Nonlinear Optical Material Discovered by the Combination of Electron Diffraction and First-Principles Calculations. Chemistry of Materials, 2018, 30, 2203-2207.	6.7	39
83	Hydroxyl free radical route to the stable siliceous Ti-UTL with extra-large pores for oxidative desulfurization. Chemical Communications, 2019, 55, 1390-1393.	4.1	39
84	Structure determination of the zeolite IM-5 using electron crystallography. Zeitschrift Für Kristallographie, 2010, 225, 77-85.	1.1	38
85	A one-step water based strategy for synthesizing hydrated vanadium pentoxide nanosheets from VO ₂ (B) as free-standing electrodes for lithium battery applications. Journal of Materials Chemistry A, 2016, 4, 17988-18001.	10.3	38
86	Guest-Binding-Induced Interhetero Hosts Charge Transfer Crystallization: Selective Coloration of Commonly Used Organic Solvents. Journal of the American Chemical Society, 2021, 143, 1553-1561.	13.7	38
87	Catalytic Water Oxidation by a Molecular Ruthenium Complex: Unexpected Generation of a Single-Site Water Oxidation Catalyst. Inorganic Chemistry, 2015, 54, 4611-4620.	4.0	37
88	Unusual Strong Incommensurate Modulation in a Tungsten-Bronze-Type Relaxor PbBiNb ₅ O ₁₅ . Journal of the American Chemical Society, 2015, 137, 13468-13471.	13.7	37
89	Covalently linking CuInS ₂ quantum dots with a Re catalyst by click reaction for photocatalytic CO ₂ reduction. Dalton Transactions, 2018, 47, 10775-10783.	3.3	37
90	A Deepâ€UV Nonlinear Optical Borosulfate with Incommensurate Modulations. Angewandte Chemie - International Edition, 2021, 60, 11457-11463.	13.8	37

#	Article	IF	CITATIONS
91	A Cuâ€Based Nanoparticulate Film as Superâ€Active and Robust Catalyst Surpasses Pt for Electrochemical H ₂ Production from Neutral and Weak Acidic Aqueous Solutions. Advanced Energy Materials, 2016, 6, 1502319.	19.5	36
92	Divergent Chemistry Paths for 3D and 1D Metallo ovalent Organic Frameworks (COFs). Angewandte Chemie - International Edition, 2020, 59, 11527-11532.	13.8	35
93	Crystal Growth and Structure Determination of Oxygen-Deficient Sr6Co5O15. Inorganic Chemistry, 2006, 45, 8394-8402.	4.0	34
94	Pd0.213Cd0.787 and Pd0.235Cd0.765 Structures: Their Longc Axis and Composite Crystals, Chemical Twinning, and Atomic Site Preferences. Chemistry - A European Journal, 2007, 13, 1394-1410.	3.3	34
95	An intriguing intermediate state as a bridge between antiferroelectric and ferroelectric perovskites. Materials Horizons, 2020, 7, 1912-1918.	12.2	34
96	PKU-3: An HCl-Inclusive Aluminoborate for Strecker Reaction Solved by Combining RED and PXRD. Journal of the American Chemical Society, 2015, 137, 7047-7050.	13.7	33
97	Elucidation of Adsorbate Structures and Interactions on BrÃ,nsted Acid Sites in Hâ€ZSMâ€5 by Synchrotron Xâ€ray Powder Diffraction. Angewandte Chemie - International Edition, 2016, 55, 5981-5984.	13.8	33
98	A novel 1D independent metal–organic nanotube based on cyclotriveratrylene ligand. CrystEngComm, 2012, 14, 112-115.	2.6	31
99	Isostructural Threeâ€Dimensional Covalent Organic Frameworks. Angewandte Chemie, 2019, 131, 9872-9877.	2.0	31
100	Unusual Long-Range Ordering Incommensurate Structural Modulations in an Organic Molecular Ferroelectric. Journal of the American Chemical Society, 2017, 139, 15900-15906.	13.7	30
101	Paramagnetic Conducting Metal–Organic Frameworks with Threeâ€Dimensional Structure. Angewandte Chemie - International Edition, 2020, 59, 20873-20878.	13.8	30
102	Investigation of the GeO2-1,6-Diaminohexane-Water-Pyridine-HF Phase Diagram Leading to the Discovery of Two Novel Layered Germanates with Extra-Large Rings. Inorganic Chemistry, 2011, 50, 201-207.	4.0	29
103	Simple CTAB surfactant-assisted hierarchical lamellar MWW titanosilicate: a high-performance catalyst for selective oxidations involving bulky substrates. Catalysis Science and Technology, 2017, 7, 2874-2885.	4.1	28
104	A silicogermanate with 20-ring channels directed by a simple quaternary ammonium cation. Dalton Transactions, 2013, 42, 1360-1363.	3.3	27
105	Accurate structure determination of a borosilicate zeolite EMM-26 with two-dimensional 10 \tilde{A} — 10 ring channels using rotation electron diffraction. Inorganic Chemistry Frontiers, 2016, 3, 1444-1448.	6.0	27
106	Ultraquantum magnetoresistance in the Kramers-Weyl semimetal candidate βâ^'Ag2Se. Physical Review B, 2017, 96, .	3.2	27
107	3D Electron Diffraction Unravels the New Zeolite ECNUâ€23 from the "Pure―Powder Sample of ECNUâ€21. Angewandte Chemie - International Edition, 2020, 59, 1166-1170.	13.8	27
108	Epitaxial growth of core–shell zeolite X–A composites. CrystEngComm, 2012, 14, 2204.	2.6	26

#	Article	IF	CITATIONS
109	A Crystalline Mesoporous Germanate with 48â€Ring Channels for CO ₂ Separation. Angewandte Chemie - International Edition, 2015, 54, 7290-7294.	13.8	26
110	V2O5•nH2O nanosheets and multi-walled carbon nanotube composite as a negative electrode for sodium-ion batteries. Journal of Energy Chemistry, 2019, 30, 145-151.	12.9	26
111	Highly Conducting Organic–Inorganic Hybrid Copper Sulfides Cu _{<i>x</i>} C ₆ 6 (x=4 or 5.5): Ligandâ€Based Oxidationâ€Induced Chemical and Electronic Structure Modulation. Angewandte Chemie - International Edition, 2020, 59, 22602-22609.	13.8	26
112	Triptycene-based three-dimensional covalent organic frameworks with stp topology of honeycomb structure. Materials Chemistry Frontiers, 2021, 5, 944-949.	5.9	26
113	Open-Framework Germanate Built from the Hexagonal Packing of Rigid Cylinders. Inorganic Chemistry, 2009, 48, 9962-9964.	4.0	25
114	Water Oxidation Initiated by In Situ Dimerization of the Molecular Ru(pdc) Catalyst. ACS Catalysis, 2018, 8, 4375-4382.	11.2	25
115	Synthesis and Structure Determination of SCMâ€15: A 3D Large Pore Zeolite with Interconnected Straight 12×12×10â€Ring Channels. Chemistry - A European Journal, 2019, 25, 2184-2188.	3.3	25
116	SU-22 and SU-23: Layered Germanates Built from 4-Coordinated Ge ₇ Clusters Exhibiting Structural Variations on the 4 ⁴ Topology. Crystal Growth and Design, 2008, 8, 3695-3699.	3.0	24
117	Synthesis and Structure Determination of Largeâ€Pore Zeolite SCMâ€14. Chemistry - A European Journal, 2017, 23, 16829-16834.	3.3	24
118	Guest-Controlled Incommensurate Modulation in a Meta-Rigid Metal–Organic Framework Material. Journal of the American Chemical Society, 2020, 142, 19189-19197.	13.7	24
119	Rare earth elements based oxide ion conductors. Inorganic Chemistry Frontiers, 2021, 8, 1374-1398.	6.0	24
120	Fourâ€Dimensional Space Groups for Pedestrians: Composite Structures. Chemistry - an Asian Journal, 2007, 2, 1204-1229.	3.3	23
121	Soluble Silver Acetylide for the Construction and Structural Conversion of All-Alkynyl-Stabilized High-Nuclearity Homoleptic Silver Clusters. Crystal Growth and Design, 2015, 15, 2505-2513.	3.0	22
122	A luminescent Zr-based metal–organic framework for sensing/capture of nitrobenzene and high-pressure separation of CH ₄ /C ₂ H ₆ . Journal of Materials Chemistry A, 2015, 3, 23493-23500.	10.3	22
123	A ruthenium water oxidation catalyst based on a carboxamide ligand. Dalton Transactions, 2016, 45, 3272-3276.	3.3	21
124	A heavy metal-free CuInS ₂ quantum dot sensitized NiO photocathode with a Re molecular catalyst for photoelectrochemical CO ₂ reduction. Chemical Communications, 2019, 55, 7918-7921.	4.1	21
125	Flexible Freestanding MoO 3â~' x –Carbon Nanotubes–Nanocellulose Paper Electrodes for Charge‧torage Applications. ChemSusChem, 2019, 12, 5157-5163.	6.8	20
126	Modulated structure determination and ion transport mechanism of oxide-ion conductor CeNbO4+δ. Nature Communications, 2020, 11, 4751.	12.8	20

#	Article	IF	CITATIONS
127	Two Open-Framework Germanates with Nickel Complexes Incorporated into the Framework. Inorganic Chemistry, 2011, 50, 9921-9923.	4.0	19
128	Synthesis of a [3Fe2S] Cluster with Low Redox Potential from [2Fe2S] Hydrogenase Models: Electrochemical and Photochemical Generation of Hydrogen. European Journal of Inorganic Chemistry, 2011, 2011, 1100-1105.	2.0	19
129	Acetonitrileâ€Based Electrolytes for Rechargeable Zinc Batteries. Energy Technology, 2020, 8, 2000358.	3.8	19
130	A 3D 12â€Ring Zeolite with Ordered 4â€Ring Vacancies Occupied by (H ₂ O) ₂ Dimers. Chemistry - A European Journal, 2014, 20, 16097-16101.	3.3	17
131	Superconductivity in Perovskite Ba _{1–<i>x</i>} Ln _{<i>x</i>} (Bi _{0.20} Pb _{0.80})O _{3â^îî} (Ln = La, Ce, Pr, Nd, Sm, Eu, Gd, Tb, Dy, Ho, Er, Tm, Yb, Lu). Inorganic Chemistry, 2018, 57, 1269-1276.	4.0	17
132	Discovery of Complex Metal Oxide Materials by Rapid Phase Identification and Structure Determination. Journal of the American Chemical Society, 2019, 141, 4990-4996.	13.7	17
133	IDMâ€1: A Zeolite with Intersecting Medium and Extraâ€Large Pores Built as an Expansion of Zeolite MFI. Angewandte Chemie - International Edition, 2020, 59, 11283-11286.	13.8	17
134	Binding and separation of CO ₂ , SO ₂ and C ₂ H ₂ in homo- and hetero-metallic metal–organic framework materials. Journal of Materials Chemistry A, 2021, 9, 7190-7197.	10.3	17
135	A ₂ SnS ₅ : A Structural Incommensurate Modulation Exhibiting Strong Secondâ€Harmonic Generation and a High Laserâ€Induced Damage Threshold (A=Ba, Sr). Angewandte Chemie, 2020, 132, 11959-11963.	2.0	17
136	Oneâ€Step Catalytic Enantioselective αâ€Quaternary 5â€Hydroxyproline Synthesis: An Asymmetric Entry to Highly Functionalized αâ€Quaternary Proline Derivatives. Advanced Synthesis and Catalysis, 2012, 354, 1156-1162.	4.3	16
137	Achiral Coâ€Catalyst Induced Switches in Catalytic Asymmetric Reactions on Racemic Mixtures (RRM): From Stereodivergent RRM to Stereoconvergent Deracemization by Combination of Hydrogen Bond Donating and Chiral Amine Catalysts. Advanced Synthesis and Catalysis, 2012, 354, 2865-2872.	4.3	15
138	Construct Polyoxometalate Frameworks through Covalent Bonds. Inorganic Chemistry, 2015, 54, 8699-8704.	4.0	15
139	Hierarchical Shellâ€Like ZSMâ€5 with Tunable Porosity Synthesized by using a Dissolution–Recrystallization Approach. Chemistry - A European Journal, 2018, 24, 14974-14981.	3.3	15
140	HPMâ€14: A New Germanosilicate Zeolite with Interconnected Extraâ€Large Pores Plus Oddâ€Membered and Small Pores**. Angewandte Chemie - International Edition, 2021, 60, 3438-3442.	13.8	15
141	Structure–direction towards the new large pore zeolite NUD-3. Chemical Communications, 2021, 57, 191-194.	4.1	15
142	Structure determination of zeolites and ordered mesoporous materials by electron crystallography. Dalton Transactions, 2010, 39, 8355.	3.3	14
143	Elucidation of Adsorbate Structures and Interactions on BrÃ,nsted Acid Sites in Hâ€ZSMâ€5 by Synchrotron Xâ€ray Powder Diffraction. Angewandte Chemie, 2016, 128, 6085-6088.	2.0	14
144	A Water Based Synthesis of Ultrathin Hydrated Vanadium Pentoxide Nanosheets for Lithium Battery Application: Free Standing Electrodes or Conventionally Casted Electrodes?. Electrochimica Acta, 2017, 252, 254-260.	5.2	14

#	Article	IF	CITATIONS
145	Synthesis, structure, and superconductivity of B-site doped perovskite bismuth lead oxide with indium. Inorganic Chemistry Frontiers, 2020, 7, 3561-3570.	6.0	14
146	Design and Synthesis of a Zeolitic Organic Framework**. Angewandte Chemie - International Edition, 2022, 61, .	13.8	14
147	Construction of 3-fold interpenetrated pcu organic frameworks from methanetetrabenzoic acid with zigzag bipyridines. CrystEngComm, 2009, 11, 2277.	2.6	13
148	BiMnFe2O6, a polysynthetically twinned hcp MO structure. Chemical Science, 2010, 1, 751.	7.4	13
149	SU-62: Synthesis and Structure Investigation of a Germanate with a Novel Three-Dimensional Net and Interconnected 10- and 14-Ring Channels. Crystal Growth and Design, 2012, 12, 369-375.	3.0	13
150	Disorder in Extra-Large Pore Zeolite ITQ-33 Revealed by Single Crystal XRD. Crystal Growth and Design, 2013, 13, 4168-4171.	3.0	13
151	Layered V–B–O polyoxometalate nets linked by diethylenetriamine complexes with dangling amine groups. Dalton Transactions, 2014, 43, 15283-15286.	3.3	13
152	Undulated 2D Covalent Organic Frameworks Based on Bowlâ€ S haped Cyclotricatechylene. Chinese Journal of Chemistry, 2016, 34, 783-787.	4.9	13
153	Structure modulations in nonlinear optical (NLO) materials Cs2TB4O9(T= Ge, Si). Acta Crystallographica Section B: Structural Science, Crystal Engineering and Materials, 2016, 72, 194-200.	1.1	13
154	Synthesis and characterization of germanosilicate molecular sieves: GeO ₂ /SiO ₂ ratio, H ₂ O/TO ₂ ratio and temperature. Dalton Transactions, 2017, 46, 2270-2280.	3.3	13
155	Synthesis, structure and magnetic properties of (Eu1â^'xMnx)MnO3â^'δ. RSC Advances, 2017, 7, 2019-2024.	3.6	13
156	A complicated quasicrystal approximant â^Š ₁₆ predicted by the strong-reflections approach. Acta Crystallographica Section B: Structural Science, 2010, 66, 17-26.	1.8	12
157	Approaching the structure of REBaB9O16 (RE = rare earth) by characterization of a new analogue Ba6Bi9B79O138. Journal of Materials Chemistry C, 2015, 3, 4431-4437.	5.5	12
158	A multi-dimensional quasi-zeolite with 12 × 10 × 7-ring channels demonstrates high thermal stability and good gas adsorption selectivity. Chemical Science, 2016, 7, 3025-3030.	7.4	12
159	Insights into the Exfoliation Process of V ₂ O ₅ · <i>n</i> H ₂ O Nanosheet Formation Using Real-Time ⁵¹ V NMR. ACS Omega, 2019, 4, 10899-10905.	3.5	12
160	IDMâ€∃: A Zeolite with Intersecting Medium and Extra‣arge Pores Built as an Expansion of Zeolite MFI. Angewandte Chemie, 2020, 132, 11379-11382.	2.0	12
161	Phase Equilibrium of the In2O3â^'TiO2â^'MO (M = Ca, Sr) Systems and the Structure of In6Ti6CaO22. Chemistry of Materials, 2005, 17, 2186-2192.	6.7	11
162	Enhancement of Ferroelectricity for Orthorhombic (Tb _{0.861} Mn _{0.121})MnO _{3â^îî} by Copper Doping. Inorganic Chemistry, 2017, 56, 3475-3482.	4.0	11

#	Article	IF	CITATIONS
163	Crystallization of a Novel Germanosilicate ECNUâ€16 Provides Insights into the Spaceâ€Filling Effect on Zeolite Crystal Symmetry. Chemistry - A European Journal, 2018, 24, 9247-9253.	3.3	11
164	A Deepâ€UV Nonlinear Optical Borosulfate with Incommensurate Modulations. Angewandte Chemie, 2021, 133, 11558-11564.	2.0	11
165	EMM-25: The Structure of Two-Dimensional 11 × 10 Medium-Pore Borosilicate Zeolite Unraveled Using 3D Electron Diffraction. Chemistry of Materials, 2021, 33, 4146-4153.	6.7	11
166	Tailoring the Pore Surface of 3D Covalent Organic Frameworks via Postâ€&ynthetic Click Chemistry. Angewandte Chemie, 2022, 134, .	2.0	11
167	The Structure of a Complex Open-Framework Germanate Obtained by Combining Powder Charge-Flipping and Simulated Annealing. Crystal Growth and Design, 2012, 12, 4853-4860.	3.0	10
168	Alkene Epoxidation Catalysts [Ru(pdc)(tpy)] and [Ru(pdc)(pybox)] Revisited: Revealing a Unique Ru ^{IV} â•O Structure from a Dimethyl Sulfoxide Coordinating Complex. ACS Catalysis, 2015, 5, 3966-3972.	11.2	10
169	Structure determination of modulated structures by powder X-ray diffraction and electron diffraction. Inorganic Chemistry Frontiers, 2016, 3, 1351-1362.	6.0	10
170	Superconductivity of Perovskite Ba1â´'x Y x (Bi0.2Pb0.8)O3â´Î´. Journal of Superconductivity and Novel Magnetism, 2017, 30, 1705-1712.	1.8	10
171	Divergent Chemistry Paths for 3D and 1D Metalloâ€Covalent Organic Frameworks (COFs). Angewandte Chemie, 2020, 132, 11624-11629.	2.0	10
172	Atomic-resolution structures from polycrystalline covalent organic frameworks with enhanced cryo-cRED. Nature Communications, 2022, 13, .	12.8	10
173	One dimensional infinite water wires incorporated in isostructural organic crystalline supermolecules with zwitterionic channels. CrystEngComm, 2011, 13, 1287-1290.	2.6	9
174	Three low-dimensional open-germanates based on the 44 net. CrystEngComm, 2012, 14, 5465.	2.6	9
175	Stepwise tuning of the substituent groups from mother BTB ligands to two hexaphenylbenzene based ligands for construction of diverse coordination polymers. CrystEngComm, 2013, 15, 8511.	2.6	9
176	Germanate with Three-Dimensional 12 × 12 × 11-Ring Channels Solved by X-ray Powder Diffraction with Charge-Flipping Algorithm. Inorganic Chemistry, 2013, 52, 10238-10244.	4.0	9
177	Stomata-like metal peptide coordination polymer. Journal of Materials Chemistry A, 2017, 5, 23440-23445.	10.3	9
178	Photoinduced synthesis of Bi ₂ O ₃ nanotubes based on oriented attachment. Journal of Materials Chemistry A, 2019, 7, 1424-1428.	10.3	9
179	Crystal structure and optical performance analysis of a new type of persistent luminescence material with multi-functional application prospects. Journal of Energy Chemistry, 2022, 69, 150-160.	12.9	9
180	Achieving ultrahigh electrochemical performance by surface design and nanoconfined water manipulation. National Science Review, 2022, 9, .	9.5	9

#	Article	IF	CITATIONS
181	An Open-Framework Aluminophosphite with Face-Sharing AlO ₆ Octahedra Dimers and Extra-Large 14-Ring Channels. Crystal Growth and Design, 2018, 18, 1267-1271.	3.0	8
182	3D Electron Diffraction Unravels the New Zeolite ECNUâ€23 from the "Pure―Powder Sample of ECNUâ€21. Angewandte Chemie, 2020, 132, 1182-1186.	2.0	8
183	An Intriguing Polarization Configuration of Mixed Ising- and Néel-Type Model in the Prototype PbZrO ₃ -Based Antiferroelectrics. Inorganic Chemistry, 2021, 60, 3232-3237.	4.0	8
184	Borates as a new direction in the design of oxide ion conductors. Science China Materials, 2022, 65, 2737-2745.	6.3	8
185	Supra-molecular assembly of aromatic proton sponges to direct the crystallization of extra-large-pore zeotypes. Proceedings of the Royal Society A: Mathematical, Physical and Engineering Sciences, 2014, 470, 20140107.	2.1	7
186	Topotactic Reduction toward a Noncentrosymmetric Deficient Perovskite Tb _{0.50} Ca _{0.50} Mn _{0.96} O _{2.37} with Ordered Mn Vacancies and Piezoelectric Behavior. Chemistry of Materials, 2017, 29, 9840-9850.	6.7	7
187	Synthesis and crystal structure of Sr ₃ Bi ₂ O ₆ and structural change in the strontium–bismuth-oxide system. Dalton Transactions, 2018, 47, 1888-1894.	3.3	7
188	A Facile and Green Method for the Synthesis of SFE Borosilicate Zeolite and Its Heteroatom‧ubstituted Analogues with Promising Catalytic Performances. Chemistry - A European Journal, 2018, 24, 306-311.	3.3	7
189	Synthesis and Structure of a Layered Fluoroaluminophosphate and Its Transformation to a Three-Dimensional Zeotype Framework. Inorganic Chemistry, 2018, 57, 11753-11760.	4.0	7
190	One-pot synthesis of Cu-modified HNb ₃ O ₈ nanobelts with enhanced photocatalytic hydrogen production. Journal of Materials Chemistry A, 2018, 6, 10769-10775.	10.3	7
191	Superconductivity in Perovskite Ba _{1â^x} K _x Bi _{0.30} Pb _{0.70} O _{3â^î^} . ChemistrySelect, 2019, 4, 3135-3139.	1.5	7
192	An NHC-CuCl functionalized metal–organic framework for catalyzing β-boration of α,β-unsaturated carbonyl compounds. Dalton Transactions, 2019, 48, 5144-5148.	3.3	7
193	Stable, Efficient, Copper Coordination Polymer-Derived Heterostructured Catalyst for Oxygen Evolution under pH-Universal Conditions. ACS Applied Materials & Interfaces, 2021, 13, 25461-25471.	8.0	7
194	SU-75: a disordered Ge10 germanate with pcu topology. Dalton Transactions, 2012, 41, 12358.	3.3	6
195	SU-79: a novel germanate with 3D 10- and 11-ring channels templated by a square-planar nickel complex. Inorganic Chemistry Frontiers, 2014, 1, 278-283.	6.0	6
196	Multiferroicity Broken by Commensurate Magnetic Ordering in Terbium Orthomanganite. ChemPhysChem, 2016, 17, 1098-1103.	2.1	6
197	A crystalline AlPO4-5 intermediate: designed synthesis, structure, and phase transformation. Dalton Transactions, 2017, 46, 12209-12216.	3.3	6
198	Highly Diastereo―and Enantioselective Cascade Synthesis of Bicyclic Lactams in Oneâ€Pot. European Journal of Organic Chemistry, 2018, 2018, 1158-1164.	2.4	6

#	Article	IF	CITATIONS
199	Room Temperature Zero Thermal Expansion in a Cubic Cobaltite. Journal of Physical Chemistry Letters, 2020, 11, 6785-6790.	4.6	6
200	Guest-Induced Switching of a Molecule-Based Magnet in a 3d–4f Heterometallic Cluster-Based Chain Structure. Inorganic Chemistry, 2021, 60, 633-641.	4.0	6
201	PKU-20: A new silicogermanate constructed from sti and asv layers. Microporous and Mesoporous Materials, 2016, 224, 384-391.	4.4	5
202	Hydrothermal assembly of various dimensional pure-inorganic copper–molybdenum frameworks. CrystEngComm, 2016, 18, 521-524.	2.6	5
203	Nonmetallic metal toward a pressure-induced bad-metal state in two-dimensional Cu ₃ LiRu ₂ O ₆ . Chemical Communications, 2020, 56, 265-268.	4.1	5
204	Nonâ€Interpenetrated Singleâ€Crystal Covalent Organic Frameworks. Angewandte Chemie, 2020, 132, 18147-18151.	2.0	5
205	HPMâ€14: A New Germanosilicate Zeolite with Interconnected Extraâ€Large Pores Plus Oddâ€Membered and Small Pores**. Angewandte Chemie, 2021, 133, 3480-3484.	2.0	5
206	SCM-25: A Zeolite with Ordered Meso-cavities Interconnected by 12Â×Â12Â×Â10-Ring Channels Determined 3D Electron Diffraction. Inorganic Chemistry, 2022, 61, 4371-4377.	^{by} 4.0	5
207	DMAP-Induced Gallium Phosphites with Different Dimensionality. Crystal Growth and Design, 2019, 19, 6011-6016.	3.0	4
208	An Interrupted Zeolite PKUâ€26 and Its Transformation to a Fully Fourâ€Connected Zeolite PKUâ€27 upon Calcination. Chemistry - A European Journal, 2019, 25, 3219-3223.	3.3	4
209	Superconductivity in Perovskite Ba0.85â^'xLaxPr0.15(Bi0.20Pb0.80)O3â^'δ. Journal of Superconductivity and Novel Magnetism, 2019, 32, 167-173.	1.8	4
210	Paramagnetic Conducting Metal–Organic Frameworks with Threeâ€Dimensional Structure. Angewandte Chemie, 2020, 132, 21059-21064.	2.0	4
211	Rational Manipulation of Stacking Arrangements in Threeâ€Đimensional Zeolites Built from Twoâ€Đimensional Zeolitic Nanosheets. Angewandte Chemie - International Edition, 2020, 59, 19934-19939.	13.8	4
212	Structure determination of [3Fe2S] complex with complicated pseudo-merohedric twinning. Zeitschrift Für Kristallographie, 2012, 227, 221-226.	1.1	3
213	Three-Dimensional Open-Framework Germanate Built from a Novel Ge ₁₃ Cluster and Containing Two Types of Chiral Layers. Crystal Growth and Design, 2018, 18, 928-933.	3.0	3
214	Mechanistic Insights into Solid-State p-Type Dye-Sensitized Solar Cells. Journal of Physical Chemistry C, 2019, 123, 26151-26160.	3.1	3
215	Quasicrystal-related mosaics with periodic lattices interlaid with aperiodic tiles. Acta Crystallographica Section A: Foundations and Advances, 2020, 76, 137-144.	0.1	3
216	Volcanic relationship between wettability of the interface and water migration rate in solar steam generation systems. Nano Research, 0, , 1.	10.4	3

#	Article	IF	CITATIONS
217	Elucidation of correlated disorder in zeolite IM-18. Acta Crystallographica Section B: Structural Science, Crystal Engineering and Materials, 2019, 75, 333-342.	1.1	3
218	Crystalline Sponge Method by Three-Dimensional Electron Diffraction. Frontiers in Molecular Biosciences, 2021, 8, 821927.	3.5	3
219	Accurate structure determination of nanocrystals by continuous precession electron diffraction tomography. Science China Materials, 2022, 65, 1417-1420.	6.3	3
220	Mullite-derivative Bi2MnxAl7â^'xO14 (xâ^¼ 1): structure determination by powder X-ray diffraction from a multi-phase sample. Dalton Transactions, 2012, 41, 2884.	3.3	2
221	Synthesis, Structure, and Properties of the Non-Centrosymmeteric Compound LiNaRbB ₅ O ₈ (OH) ₂ . Crystal Growth and Design, 2018, 18, 5745-5749.	3.0	2
222	A New Layered Silicogermanate PKU-23 and Its Transformation to a Zeolite with Three-Dimensional Channels. Crystal Growth and Design, 2019, 19, 2272-2278.	3.0	2
223	Synthesis and characterizations of TiN–SBA-15 mesoporous materials for CO ₂ dry reforming enhancement. Pure and Applied Chemistry, 2020, 92, 545-556.	1.9	2
224	Highly Conducting Organic–Inorganic Hybrid Copper Sulfides Cu x C 6 S 6 (x=4 or 5.5): Ligandâ€Based Oxidationâ€Induced Chemical and Electronic Structure Modulation. Angewandte Chemie, 2020, 132, 22791-22798.	2.0	2
225	Synthesis of crystalline WS ₃ with a layered structure and desert-rose-like morphology. Nanoscale Advances, 2022, 4, 1626-1631.	4.6	2
226	Collective and individual impacts of the cascade doping of alkali cations in perovskite single crystals. Journal of Materials Chemistry C, 2020, 8, 15351-15360.	5.5	1
227	A general method for searching for homometric structures. Acta Crystallographica Section B: Structural Science, Crystal Engineering and Materials, 2022, 78, 14-19.	1.1	1
228	Constructing Concentration and Temperature Controllable Blue-Green Emission in a Single-Component Solid-State Phosphor. Journal of Physical Chemistry C, 2021, 125, 27420-27428.	3.1	1
229	Quantitative Electron Diffraction for Crystal Structure Determination. Materials Research Society Symposia Proceedings, 2009, 1184, 31.	0.1	0
230	Rücktitelbild: A Tailor-Made Molecular Ruthenium Catalyst for the Oxidation of Water and Its Deactivation through Poisoning by Carbon Monoxide (Angew. Chem. 15/2013). Angewandte Chemie, 2013, 125, 4370-4370.	2.0	0
231	Rücktitelbild: Elucidation of Adsorbate Structures and Interactions on BrÃ,nsted Acid Sites in Hâ€ZSMâ€5 by Synchrotron Xâ€ray Powder Diffraction (Angew. Chem. 20/2016). Angewandte Chemie, 2016, 128, 6214-6214.	2.0	0
232	Innenrücktitelbild: Self-Supporting Metal-Organic Layers as Single-Site Solid Catalysts (Angew. Chem.) Tj ETQo	9.0 g rgB 2.9 rgB	BT /Qverlock 1
	Electro setalusia: Hierarchical Co(OH)E Superstructure Built bul ou î 6 Dimensional Substructures for		

Electrocatalytic Water Oxidation (Adv. Mater. 28/2017). Advanced Materials, 2017, 29, .

²³⁴PKUâ€21: A Novel Layered Germanate Built from Ge₇ and Ge₁₀ Clusters for
CO₂ Separation. Chemistry - A European Journal, 2017, 23, 17879-17884.3.3

#	Article	IF	CITATIONS
235	Frontispiece: A Facile and Green Method for the Synthesis of SFE Borosilicate Zeolite and Its Heteroatom‣ubstituted Analogues with Promising Catalytic Performances. Chemistry - A European Journal, 2018, 24, .	3.3	0
236	Effect of zinc doping on structural, magnetic and dielectric properties of perovskite (Tb0.874Mn0.106)MnO3â~δ. Journal of Materials Science: Materials in Electronics, 2018, 29, 16543-16552.	2.2	0
237	Discovery of Layered Indium Hydroxide via a Hydroperoxyl Anion Coordinated Precursor at Room Temperature. Chemistry - A European Journal, 2018, 24, 15491-15494.	3.3	0
238	Synthesis, characterization and structure of (NH ₄) ₄ [Zn ₅ VIV4VV16O ₅₆ H ₂ (H ₂ with a novel V ₅ O ₁₄ layer. Dalton Transactions, 2019, 48, 4906-4911.	0)3 .s ub>4	ł Ωub]
239	Rational Manipulation of Stacking Arrangements in Threeâ€Dimensional Zeolites Built from Twoâ€Dimensional Zeolitic Nanosheets. Angewandte Chemie, 2020, 132, 20106-20111.	2.0	0
240	Design and Synthesis of a Zeolitic Organic Framework. Angewandte Chemie, 0, , .	2.0	0
241	Synthesis, Structure and Superconducting Properties of Ba1-xLax/4K3x/4(Bi0.25Pb0.75)O3- Perovskites. Physica C: Superconductivity and Its Applications, 2022, 598, 1354075.	1.2	0